Annals of R.S.C.B., ISSN:1583-6258, Vol. 25, Issue 6, 2021, Pages. 12715 - 12725
Received 25 April 2021; Accepted 08 May 2021.

Monte Carlo Dose Calculation around the Isoseed® I25.S06 Brachytherapy Source in Water and in Different Media Using Gate 8.2

Lahcen Ait-Mlouk[1], Mohammed Khalis[1], Hmad Ouabi[2], Hassan Asnaoui[1], Said Elboukhari[3]

[1]Moulay Ismail University, Faculty of Sciences, Department of Physics (N.T.P.T), Meknes, Morocco
[2]Oncology Centre Al Azhar, Rabat, Morocco
[3]Moulay Ismail University, Faculty of Sciences, Department of Chemistry, Meknes, Morocco
E-mail: mloukylahcen@gmail.com

ABSTRACT

Low dose rate (LDR) brachytherapy is widely used in treating tumors, including the brain, the eye tumors and the prostate cancer. Dosimetric characteristics of brachytherapy source before the clinical application are crucial as recommended by the American Association of Physicists in Medicine (AAPM). In the presented study, two dosimetric parameters of the iodine-125 (^{125}I) model IsoSeed®I25.S06 source were calculated around a low dose rate ^{125}I source located in a spherical phantom with radius of 15.0 cm using GEANT4 Application for Emission Tomography Monte Carlo code (version 8.2). As a result, we have obtained the radial dose function $g_L(r)$ and the anisotropy function $F(r, \theta)$ in water. Moreover, to highlight the effect of media composition on the dose distribution, the radial dose function was obtained in different media, such as adipose tissue, lung, breast tissue and muscle. The obtained results were presented and compared with consensus data. These results are in good agreement with the reference data, except the values close to the end of the source for the anisotropy functions. The radial dose function is in a good deal with consensus data, especially for $r>0.5$ cm. In addition, the radial dose function was presented for the comparison between the dose distribution in water and different tissues. This study shows a small difference between the obtained results compared to the water. Especially in long distances from the source centre due to the atomic composition and densities, which may cause errors in the estimation of the dose around brachytherapy sources that are not taken into account by Task groupn.43 (AAPM). Thus, the ignorance of atomic composition and densities, by treatment planning systems incorporates a significant error in dose delivery to the patient with Low-energy photon sources.

Keywords: Brachytherapy; Task groupn.43; GEANT4; Anisotropy function; Radial dose function.

1 INTRODUCTION

Low dose rate (LDR) brachytherapy is a technique of irradiation for cancer treatment. It involves placing radioactive sources inside tumor or as close as possible (Russell and Blasko, 1993). This technique is a modality of radiation therapy that is used for cancer treatment, more extensively employed today for the treatment of cancers including malignant the brain tumors, the eye and localized prostate cancer (Solberg et *al.*, 2002). Permanent implants have also been used for partial breast for early-stage breast cancer (Brian et *al.*, 2005). The success of this treatment modality is partly attributable to advances in the dosimetric evaluation of brachytherapy sources, the development of ultrasound guidance technology for more accurate source positioning, sophisticated treatment planning software, and minimizing the dose to surrounding normal tissues, which have ultimately translated into better clinical outcomes, compared to the external beam.

Annals of R.S.C.B., ISSN:1583-6258, Vol. 25, Issue 6, 2021, Pages. 12715 - 12725
Received 25 April 2021; Accepted 08 May 2021.

A large number of low-energy photon-emitting radioactive source models are available for radiation oncology, the most commonly used sources for LDR brachytherapy for routine clinical treatments are ^{103}Pd and ^{131}Cs as well as ^{125}I. The ^{125}I brachytherapy source are available in different physical and geometrical features, like Amersham model 6711, Amersham model 6702, Inter-source125, Best Medical Model 2301, PharmaSeed model BT-125, IsoSeed® I25.S06, etc (Heintz et *al*.,2001; Wallace, 2000). One of the most important moot points in brachytherapy, as an external radiotherapy technique is dose distribution (Williamson, 1998). The successful and effective treatment with a lesser side effect for healthy tissue depends on the dose distribution in tumors and surrounding healthy tissues. Hence, the accuracy of the dose calculations in brachytherapy is paramount (Khan and Gibbons, 2014; Allahverdi et *al.*, 2012).

The AAPM TG-43 report provides dose calculation formulas and dose parameters for brachytherapy (Rivard et *al.*, 2004). The dosimetric parameters can be evaluated by using Monte Carlo (MC) simulations and experimental methods. The MC techniques have been proposed as one of the alternatives for their ability to accurately transport low energy photons (Carrier et *al.*, 2007). It also very useful in the investigation of the dose distribution around the source, especially close to the source with a high-dose gradient (Yue, 2006). Indeed, TG-43 report does not consider both patient heterogeneities and finite patient dimensions effects, and, hence, the dose cannot be assessed accurately. This approach could result in tumor recurrence or severe side effects in healthy tissues. Therefore, investigation of dosimetric parameters in different media is an alternative to optimize the dose distribution in tumors and surrounded tissues. Several researchers used a dosimeter and MC codes to investigate the dose distribution around the brachytherapy source such as FLUKA (Rajabi and Taherparvar, 2019), MCNP (Forster et *al.*, 2004), EGS (Nelson et *al.*, 1985) and GATE/GEANT4 (Agostinelli et *al*., 2003).

The main purpose of this research study is to use the GATE (GEANT4 Application for Emission Tomography) MC code to calculate the radial dose function $g_L(r)$ and the anisotropy function $F(r, \theta)$ of IsoSeed® I25.S06 in water according to the TG-43 report. We also calculated the radial dose function in different tissues to highlight the effect of media composition on the dose distribution. The calculated values were compared with the obtained results in the water phantom. We also compared the radial dose function $g_L(r)$ with other studies in which the authors have used other available sources and MC codes.

2 MATERIALS AND METHODS

2.1 Geometry design and source description

The ^{125}I LDR brachytherapy source, model IsoSeed® I25.S06 was manufactured by BEBIG and simulated in this study using GATE 8.2 code, as shown in Figure 1. This source is similar to the UroMed/BebigSymmetra Seed model I25.S06, both in design and materials except for a small difference in physical length (4.5 mm vs 4.56 mm in length for the old one). The source capsule consists of a 0.05 mm thick titanium tube, with a density of 4.54 g.cm^{-3}. The source is sealed by laser welding using two titanium hemispherical shaped end welds, with 0.4 mm thick each. The radioactive seed core consists of a cylindrical porous ceramic (2.88 g.cm^{-3}) which is composed of alumina (Al_2O_3). The outer and inner diameters are 0.60 and 0.22 mm, respectively, and an active length of 3.50 mm. The ^{125}I atoms are assumed to be distributed uniformly. The space between the cylindrical ceramic and titanium encapsulated is filled with air. A gold rod marker (19.32 g.cm^{-3}) placed inside the ceramic core, with 3.5 mm long and 0.17 mm diameter, serves as a radio-opaque marker.

Annals of R.S.C.B., ISSN:1583-6258, Vol. 25, Issue 6, 2021, Pages. 12715 - 12725
Received 25 April 2021; Accepted 08 May 2021.

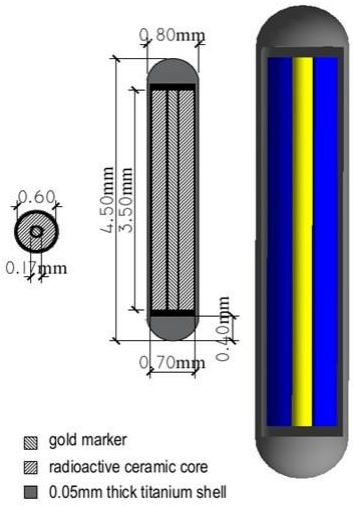

Figure 1: Schematic view for IsoSeed® I25.S06 brachytherapy seed and simulated capsule by GATE 8.2

2.2 Dosimetric parameters

According to the methodology developed by the AAPM Task Group No.43 (Nath et *al.*,1995) and its updated (TG-43U1) in 2004 (Rivard et *al.*,2004). The dose rate distribution at the point P(r, θ) can be defined in terms of polar coordinate system by Equation 1:

$$D(r,\theta) = S_k . \Lambda . \frac{G_L(r,\theta)}{G_L(r_0,\theta_0)} . g_L(r) . F(r,\theta) \quad [1]$$

Where S_k is the air-kerma strength of the source (U), Λ is the dose rate constant (cGy h^{-1} U^{-1}). $G_L(r, \theta)$ is the geometry factor. F(r, θ) is the anisotropy function and $g_L(r)$ is the radial dose function. The point P($r_0 = 1cm, \theta_0 = 90^\circ$) is chosen as a reference located in the transverse axis of the source. L is the length of the active core, r is the radial distance, θ the angle and β as showed in the Figure 2.

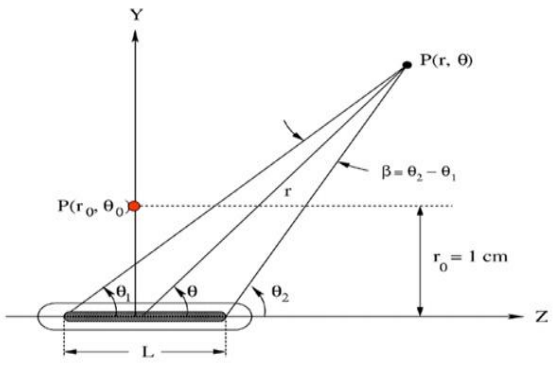

Figure 2: Coordinate system used in this study for brachytherapy dosimetry calculations.

The radial dose function $g_L(r)$ describes the attenuation of the photons in the medium along the source transverse axis ($\theta_0 = \frac{\pi}{2}$). This dosimetric function is defined as Equation 2:

$$g_L(r) = \frac{\acute{D}(r,\theta_0)}{\acute{D}(r_0,\theta_0)} \frac{G_L(r_0,\theta_0)}{G_L(r,\theta_0)} \quad (2)$$

The anisotropy function F(r, θ) describes the variation in dose around a brachytherapy source due to self-absorption and oblique filtration of radiation in the capsule material. This function is defined in Equation 3:

Annals of R.S.C.B., ISSN:1583-6258, Vol. 25, Issue 6, 2021, Pages. 12715 - 12725
Received 25 April 2021; Accepted 08 May 2021.

$$F(r,\theta) = \frac{\acute{D}(r,\theta)}{\acute{D}(r,\theta_0)} \frac{G_L(r,\theta_0)}{G_L(r,\theta)} \quad (3)$$

In this work, a line source approximation has been adopted for the geometrical factor definition. It evaluates the spatial distribution of activity along the source. A detailed description can be found in TG-43U1 report (Rivard et *al.*, 2004). The geometry function $G_L(r,\theta)$ defined by:

$$G_L(r,\theta) = \frac{tan^{-1}\left[\frac{rcos\,(\theta)+\frac{L}{2}}{rsin\,(\theta)}\right] - tan^{-1}\left[\frac{rcos\,(\theta)-\frac{L}{2}}{rsin\,(\theta)}\right]}{Lrsin\,(\theta)} \quad (4)$$

2.3 Monte Carlo calculation

The GATE Monte Carlo code was developed by international OpenGATE collaboration, based on the GEANT4 toolkit, its application areas include medical imaging devices (PET, SPECT) (Strulab et *al.*, 2003; Cuplov et *al.*, 2014), radiation therapy and dosimetry applications (Jan et *al.*, 2011). Its characteristics have been extensively discussed elsewhere (Sarrut et *al.*, 2014).

A single source model IsoSeed®I25.S06 manufactured by BEBIG was located in the center of the spherical water phantom (0.998 g.cm^{-1}) with a 15.0 cm radius according to the recommendation of the AAPM. The GATE v8.2 MC code was used to determine the radial dose function $g_L(r)$ at radial distances of 0.1–10.0 cm from the source and the anisotropy function $F(r,\theta)$ over the 0 to $\pi/2$ and 0 to 7 cm range in the longitudinal axis. Furthermore, we have calculated the radial dose function $g_L(r)$ in different tissues: muscle, breast tissue, lung and adipose tissue. The effect of the various tissues on the radial dose function of the ^{125}I brachytherapy source was investigated. The photon energy spectrum of ^{125}I was obtained from TG-43U1 report (Rivard et *al.*, 2004). The elemental compositions and mass densities of various tissues used in these simulations were adopted from report No.44 of the International Commission on Radiation Units and Measurements as shown in Table 1 (ICRU, 1989).

For this purpose, we have used two geometric systems to score the deposit energy and positions of interactions. Firstly, a set of concentric rings with 1 mm thickness at distances of $0.1 \leq r < 1$ cm from the source, rings with 2 mm thickness at distances of $1 \leq r \leq 2$ cm, rings with 4 mm thickness at distances of $3 \leq r \leq 4$ cm and rings with a thickness of 8 mm at distances of $5 \leq r \leq 10$ cm in order to score the dose at different distances. Then, $g_L(r)$ was calculated in water according to TG-43U1 and in different tissues. Secondly, a grid system composed of small spheres with different radii, located at a distance r from the source center, using the polar angles θ in respect to the central axis of the source. The simulated angle θ values increased from 0° to 90° in 10° angular increments. Using the output files of GATE MC simulations, the radial dose function $g_L(r)$ and the anisotropy function $F(r, \theta)$ were estimated.

Table 1: The density and elemental compositions based on the ICRU Report 44 (ICRU, 1989).

Elemental compositions	Adipose tissue	Breast tissue	Lung	Muscle
H	11.4	10.6	10.3	3.4
C	59.8	33.6	10.5	15.5
N	0.7	3.0	3.1	4.2
O	27.8	52.7	74.9	43.5
Na	0.1	0.1	0.2	0.1

Annals of R.S.C.B., ISSN:1583-6258, Vol. 25, Issue 6, 2021, Pages. 12715 - 12725
Received 25 April 2021; Accepted 08 May 2021.

Mg	-	-	-	0.2
Cl	0.1	0.2	0.3	-
P	-	-	0.2	0.2
S	0.1	0.2	0.3	0.3
K	-	-	0.2	0.4
Density(g/cm3)	0.95	1.02	1.05	1.05

3. RESULTS AND DISCUSSION

3.1 Radial dose function

From Equation 1 the values of the radial dose function, $g_L(r)$ were calculated as indicated in Table 2, the comparison was done with the consensus data (Rivard et *al.*, 2004), for the distances ranging from 0.1 to 10 cm as shown in Figure 3.

For distances greater than 0.5 cm, these values are much closer to consensus data. Furthermore, the mean difference between our results and consensus data was about 2.9%. On the other hand, the relative difference was below 3.13%, except the largest one was for the distances nearby the source (r <0.5 cm). This difference can be attributed to the higher photons attenuation at this area; it can also be explained by dose-scoring volume. Furthermore, the comparison of the simulated radial dose functions $g_L(r)$ of the IsoSeed® I25.S06 to that of other available sources at different radial distances are presented in Figure 4. As can be seen in this diagram, there is a good agreement between the GATE 8.2 results and those related to other sources. The differences might be due to the differences in design, composition and density of the materials, as well as some difference in the nuclear data of different codes.

The radial dose function $g_L(r)$ was investigated in different tissue phantoms with 30 cm diameter and presented in Table 3. The radial dose function decreased with increasing radial distance as shown in Figure 5. The radial dose function in adipose and breast tissues decreased at a slower rate than for water, whereas the function for lung and muscle decrease faster than for water due to the higher linear attenuation coefficient in lung and muscle than water (ICRU, 1989).

Figure 6 presents the ratio of $g_L(r)$ in the tissues to $g_L(r)$ in water. The difference between $g_L(r)$ tissues and $g_L(r)$ water increased with increasing the radial distance from the source center and decreasing photon energy. From 0.1 cm to 2, the ratio $g_L(r)_{tissue}/g_L(r)_{water}$ was close to 1±0.13, therefore the dose distributions were matching to that in water. At the distance 2 cm away the source, the ratio was 0.969, 0.973, 1.051 and 1.132 for lung, muscle, breast tissue and adipose tissue respectively. This indicates that the dose was underestimated by 3.1% for lung and 2.4% for muscle. The dose was overestimated by 5.1% for breast tissue and 13.2% for adipose tissue. Moreover, at 5 cm away, the ratio was 0.888, 0.903, 1.202 and 1.619 for lung, muscle, breast tissue and adipose tissue respectively. The dose was underestimated by 11.2% for lung and 9.7% for muscle. It was overestimated by 20.2% for breast tissue and 61% for adipose tissue. Thus the radial dose functions obtained in lung, muscle and water phantom is close to each other.

The obtained results indicate that the differences in the elemental compositions and mass densities of various tissues can influence the dose distribution. The values of the radial dose function in each tissue differ from the others; it indicates that the dose in water significantly differs from the dose in various tissues. This fact can be justified by comparing the mass-energy absorption coefficient of water and tissues. This effect implies that dosimetry using water as the tissue-equivalent medium may incorporate an overestimation or underestimation of the dose.

Annals of R.S.C.B., ISSN:1583-6258, Vol. 25, Issue 6, 2021, Pages. 12715 - 12725
Received 25 April 2021; Accepted 08 May 2021.

Table 2: Radial dose function, $g_L(r)$, of IsoSeed® I25.S06, obtained in this study and consensus data (Rivard et *al*., 2004).

Radial distance (cm)	GATE 8.2 (This work)	Consensus Data
0.10	1.0677	1.010
0.15	1.0829	1.018
0.25	1.0928	1.030
0.50	1.0817	1.030
0.75	1.0335	1.020
1.00	1.0000	1.000
1.50	0.9183	0.937
2.00	0.8317	0.857
3.00	0.6688	0.689
4.00	0.5225	0.538
5.00	0.4057	0.409
6.00	0.3101	0.313
7.00	0.2344	0.232
8.00	0.1765	0.176
9.00	0.1312	0.134
10.00	0.0987	0.0957

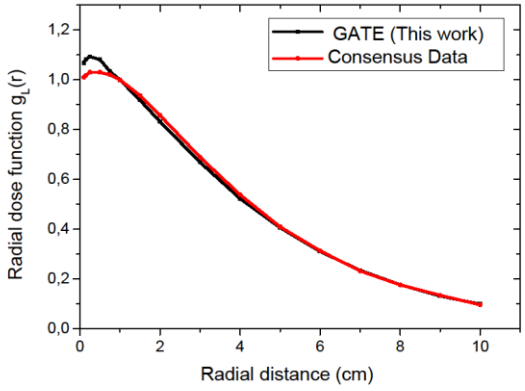

Figure 3: The comparison of the radial dose function simulation by GATE 8.2 code and consensus data for the IsoSeed®I25.S06.

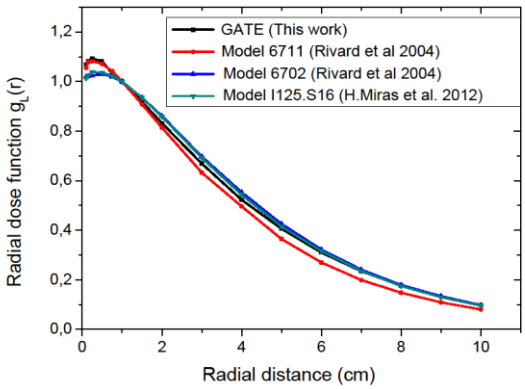

Annals of R.S.C.B., ISSN:1583-6258, Vol. 25, Issue 6, 2021, Pages. 12715 - 12725
Received 25 April 2021; Accepted 08 May 2021.

Figure 4: The Comparison between the radial dose function of the simulated IsoSeed® I25.S06 and other available sources (Rivard et *al.*, 2004).

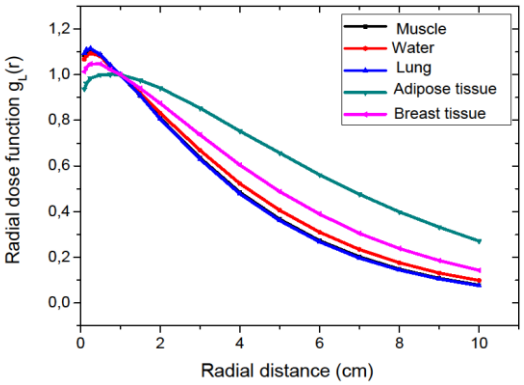

Figure 5: Radial dose function calculated by GATE 8.2 code obtained in the muscle, water, lung, adipose tissue and breast tissue.

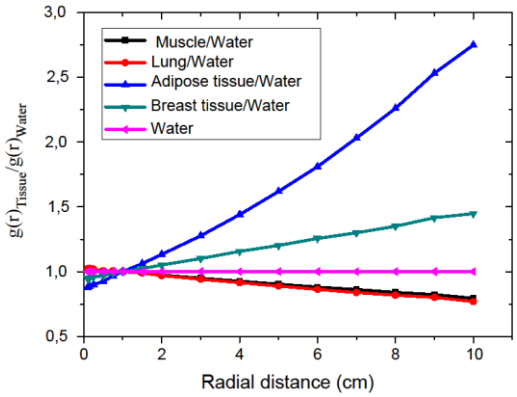

Figure 6: The ratio of $g_L(r)$ in the muscle, breast, lung and adipose tissue to $g_L(r)$ in the water.

Table 3: Radial dose function, $g_L(r)$, in different media for the IsoSeed® I25.S06, calculated by GATE 8.2 code.

Radial distance (cm)	Muscle	Lung	Adipose tissue	Breast tissue
0.1	1.0867	1.0934	0.9367	1.0133
0.15	1.1021	1.1093	0.9605	1.0309
0.25	1.1090	1.1143	0.9841	1.0469
0.5	1.0859	1.0880	0.9993	1.0472
0.75	1.0381	1.0410	1.0003	1.0215
1	1.0000	1.0000	1.0000	1.0000
1.5	0.9080	0.9092	0.9753	0.9396
2	0.8094	0.8061	0.9418	0.8744
3	0.6349	0.6295	0.8538	0.7364
4	0.4840	0.4781	0.7525	0.6044
5	0.3665	0.3605	0.6569	0.4877
6	0.2730	0.2676	0.5613	0.3895
7	0.2020	0.1965	0.4762	0.3047
8	0.1483	0.1444	0.3990	0.2384
9	0.1080	0.1051	0.3322	0.1858

Annals of R.S.C.B., ISSN:1583-6258, Vol. 25, Issue 6, 2021, Pages. 12715 - 12725
Received 25 April 2021; Accepted 08 May 2021.

10	0.0784	0.0759	0.2714	0.1429

3.2 Anisotropy function

Table 4 shows the calculated anisotropy function values by GATE 8.2 code in a water phantom, as a function of polar angle θ and radial distances.

Figure 6 illustrates a comparison between the derived anisotropy functions in this study with the consensus data. The F(r, θ) values were normalized with respect to the transverse axis of the source (θ= 90°). Those values decrease when θ approach the longitudinal axis of the source. These results show a less anisotropic dose distribution close to the source near the longitudinal axis especially for r <1 cm. For the distances from 1 to 7 cm, the values obtained show good agreement with the consensus data (Rivard et *al.*, 2004). The largest differences occur at distances close to the source, and these differences reduce while the distance increases. It can be explained by the variation in the doses distribution nearby the source, due to higher photons attenuation at this region, it could be assigned to the composition and density of the medium.

Uncertainties reported on dosimetry values calculated in this study are statistical uncertainties (type A) and do not include uncertainties in cross-sections or geometry design of the source. 10^2 photons histories were used to obtain the least uncertainties. The obtained uncertainties were 0.19% at r ≤0.5 cm and 0.38% at 0.5< r ≤10 cm for radial dose function in water and in different tissues. In the anisotropy function the statistical uncertainties less than 0.8% for all the points, except at the points located near the longitudinal axis, where it is about 1.0%. Thus, the uncertainties on the radial dose function and the anisotropy function depend on the location of calculation points as well as the size of scoring volume used and the number of histories simulated.

Table 4: Anisotropy function, F(r, θ), calculated for the IsoSeed® I25.S06 using GATE 8.2 code.

r cm θ°	0.25	0.5	1.0	2.0	3.0	4.0	5.0	7.0
0	0.3652	0.4486	0.5153	0.5565	0.6165	0.6418	0.6595	0.6974
10	0.5134	0.5130	0.5780	0.6073	0.6528	0.6964	0.7015	0.7308
20	0.7559	0.6575	0.7020	0.7312	0.7541	0.8007	0.7916	0.8024
30	0.8863	0.7858	0.8163	0.8211	0.8299	0.8634	0.8577	0.8808
40	0.9470	0.8871	0.8907	0.8703	0.8996	0.9166	0.9165	0.9205
50	0.9644	0.9438	0.9461	0.9444	0.9358	0.9629	0.9482	0.9579
60	0.9820	0.9725	0.9781	0.9476	0.9686	0.9816	0.9752	0.9770
70	1.0132	1.0010	0.9983	0.9623	0.9952	1.0048	0.9889	0.9893
80	1.0063	0.9943	0.9984	0.9702	1.0013	0.9958	0.9941	1.0229
90	1.0000	1.0000	1.0000	1.0000	1.0000	1.0000	1.0000	1.000

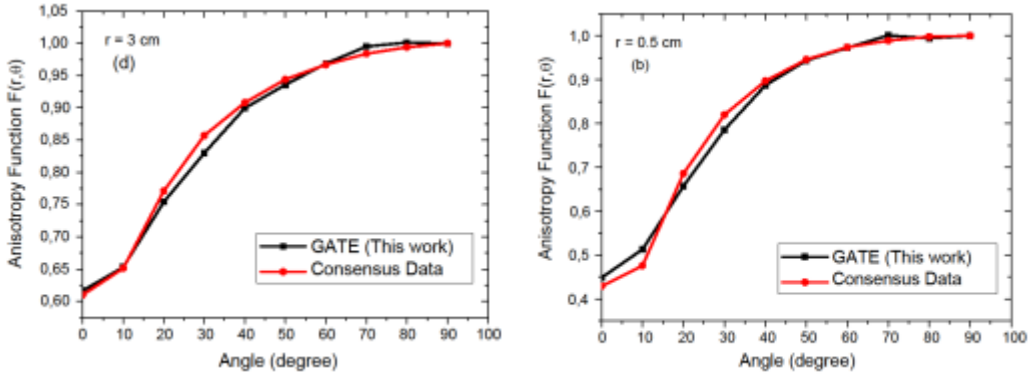

Annals of R.S.C.B., ISSN:1583-6258, Vol. 25, Issue 6, 2021, Pages. 12715 - 12725
Received 25 April 2021; Accepted 08 May 2021.

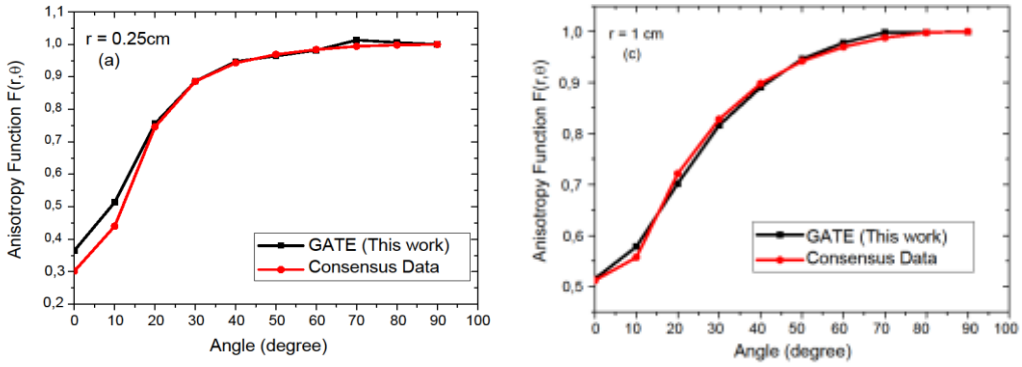

Figure 7: Calculated anisotropy function of the IsoSeed® I25.S06 compared to the consensus data at different radial distances (a), (b), (c) and (d)(Rivard et *al.*, 2004).

4. CONCLUSION

In this study, the radial dose function and anisotropy function of the ^{125}I model IsoSeed® I25.S06 have been investigated in water and different tissues using GATE (version8.2) code. The results show remarkable agreement with the consensus data, except small difference when θ approached the longitudinal axis of the source (θ<30°) and points located near the longitudinal axis especially for r = 0.25 cm. The relative difference could be explained by energy-scoring volume. It can also be partially attributed to the difference between the models of radiation transport codes.

The effect of tissue composition on dose distribution for adipose tissue, lung tissue, breast and muscle was evaluated for Iodine-125. Results show that the radial dose function in breast tissue and adipose tissue are fairly large difference in comparison with the water phantom, especially at large distances from the source center.

The overestimation or underestimation of the dose depends on the type of tissue, as well as the distance from the source. The ignorance of tissue characteristics by treatment planning systems using the TG-43 dose calculation algorithm incorporates a significant difference on dose delivery to the patient in LDR brachytherapy sources. More accurate compositions are thus important in sparing radiation sensitive healthy tissues in the vicinity of the tumors.

REFERENCE

1. Agostinelli S, Allison J, Amako K, 2003. GEANT4–a simulation toolkit. Nucl. Instrum. Meth. A, 506(25), 0.
2. Allahverdi, M., Sarkhosh, M., Aghili, M., Jaberi, R., Adelnia, A., Geraily, G., 2012. Evaluation of treatment planning system of brachytherapy according to dose to the rectum delivered. Radiation protection dosimetry, 150(3), 312-315.
3. Carrier, J. F., D'Amours, M., Verhaegen, F., Reniers, B., Martin, A. G., Vigneault, E., Beaulieu, L., 2007. Postimplant dosimetry using a Monte Carlo dose calculation engine: a new clinical standard. International Journal of Radiation Oncology* Biology* Physics, 68(4), 1190-1198.
4. Cuplov, V., Buvat, I., Pain, F., & Jan, S., 2014. Extension of the GATE Monte-Carlo simulation package to model bioluminescence and fluorescence imaging. Journal of biomedical optics, 19(2), 026004.
5. Forster, R. A., Cox, L. J., Barrett, R. F., Booth, T. E., Briesmeister, J. F., Brown, F. B., Bull, J. S., Geisler, G. C., Goorley, J. T., Russell, Post, M. D., Prael, S. E., R. E., Selcow, E. C., Sood, A., 2004. MCNP™ version 5. Nuclear Instruments and Methods in Physics Research Section B: Beam Interactions with Materials and Atoms, 213, 82-86.

6. Heintz, B. H., Wallace, R. E., Hevezi, J. M., 2001. Comparison of I-125 sources used for permanent interstitial implants. Medical physics, 28(4), 671-682.
7. ICRU, 1989. Tissue Substitutes in Radiation Dosimetry and Measurement. International Commission on Radiation Units and Measurements Report no. 44. Bethesda, MD.
8. Jan, S., Benoit, D., Becheva, E., Carlier, T., Cassol, F., Descourt, P., Frisson, T., Grevillot, L., Guigues, L., Maigne, L., Morel, C., Perrot, Y., Rehfeld, N., Sarrut, D., Schaart, D. R., Stute, S., Pietrzyk, U., Visvikis, D., Zahra, N., Buvat, I., 2011. GATE V6: a major enhancement of the GATE simulation platform enabling modelling of CT and radiotherapy. Physics in Medicine & Biology, 56(4), 881.
9. Keller, B., Sankreacha, R., Rakovitch, E., O'Brien, P., Pignol, J. P., 2005. A permanent breast seed implant as partial breast radiation therapy for early-stage patients: a comparison of palladium-103 and iodine-125 isotopes based on radiation safety considerations. International Journal of Radiation Oncology* Biology* Physics, 62(2), 358-365.
10. Khan, F. M., Gibbons, J. P., 2014. Khan's the physics of radiation therapy. Lippincott Williams & Wilkins.
11. Miras, H., Terrón, J. A., Lallena, A. M., 2013. Monte Carlo simulation of COMS ophthalmic applicators loaded with Bebig I25. S16 seeds and comparison with planning system predictions. PhysicaMedica, 29(6), 670-676.
12. Nath, R., Anderson, L. L., Luxton, G., Weaver, K. A., Williamson, J. F., &Meigooni, A. S., 1995. Dosimetry of interstitial brachytherapy sources: recommendations of the AAPM Radiation Therapy Committee Task Group No. 43. Medical physics, 22(2), 209-234.
13. Nelson, W. R., Hirayama, H., Rogers, D., 1985. The EGS4 Code System, Report SLAC-265 UC-32 (I/A).
14. Rajabi, R., &Taherparvar, P., 2019. Monte Carlo dosimetry for a new 32P brachytherapy source using FLUKA code. Journal of contemporary brachytherapy, 11(1), 76.
15. Rivard, M. J., Coursey, B. M., DeWerd, L. A., Hanson, W. F., SaifulHuq, M., Ibbott, G. S., Mitch, M. G., Nath, R., Williamson, J. F., 2004. Update of AAPM Task Group No. 43 Report: A revised AAPM protocol for brachytherapy dose calculations. Medical physics, 31(3), 633-674.
16. Russell, K.J., Blasko, J.C., 1993. Recent advances in interstitial brachytherapy for localized prostate cancer. In: Therapeutic strategies in prostate cancer. Problems in urology series. Vol. 7. Fourth edition. J. B. Lippincott Co, Philadelphia; 260-278.
17. Sarrut, D., Bardiès, M., Boussion, N., Freud, N., Jan, S., Létang, J. M., Loudos, G., Maigne, L., Marcatili, S., Mauxion, T., Papadimitroulas, P., Perrot, Y., Pietrzyk, U., Robert, C., Schaart, D., Visvikis, D., Buvat, I., 2014. A review of the use and potential of the GATE Monte Carlo simulation code for radiation therapy and dosimetry applications. Medical physics, 41(6Part1), 064301.
18. Solberg, T.D., DeMarco, J.J., Hugo, G., Wallace, R.E., 2002. Dosimetric parameters of three new solid core I-125 brachytherapy source. J ApplClin Med Phys., 3(2):119-134.
19. Strulab, D., Santin, G., Lazaro, D., Breton, V., & Morel, C., 2003. GATE (Geant4 Application for Tomographic Emission): a PET/SPECT general-purpose simulation platform. Nuclear Physics B-Proceedings Supplements, 125, 75-79.
20. Wallace, R. E., 2000, July. Dosimetric characterization of a new/sup 125/Iodine brachytherapy source, model I125-SL. In Proceedings of the 22nd Annual

Annals of R.S.C.B., ISSN:1583-6258, Vol. 25, Issue 6, 2021, Pages. 12715 - 12725
Received 25 April 2021; Accepted 08 May 2021.

International Conference of the IEEE Engineering in Medicine and Biology Society (Cat. No. 00CH37143) (Vol. 1, pp. 376-379), IEEE.
21. Williamson, J. F., 1998. Physics of brachytherapy. Principles and practice of radiation oncology, 405-468.
22. Yue, N. J., 2006. Principles and practice of brachytherapy dosimetry. Radiation measurements, 41, S22-S27.